coatings

MDPI

Article

Determination of the Coefficient of Friction in a Pulley Groove by the Indirect Method

Leopold Hrabovský *, Jiří Fries, Lukáš Kudrna and Jakub Gaszek

Department of Machine and Industrial Design, Faculty of Mechanical Engineering, VSB-Technical University of Ostrava, 70800 Ostrava, Czech Republic; jiri.fries@vsb.cz (J.F.); lukas.kudrna@vsb.cz (L.K.); jakub.gaszek.st@vsb.cz (J.G.)

* Correspondence: leopold.hrabovsky@vsb.cz; Tel.: +420-597-323-185

Abstract: In lifting systems used for the vertical transport of bulk materials and individual items or persons, so-called frictional force transmission between a steel cable and pulley is used. Due to the sufficient contact pressure between the pulley groove and the surface of the steel cable, the steel cable moves as a result of fibre friction. In general, it is possible to define fibre (also called belt) friction as the resistance that is imposed on a flexible steel cable sliding over the rounded surface of a pulley. The frictional transmission of the tractive force is considered safe if there is no slippage of the cable in the pulley groove. In the event of insufficient cable pressure against the pulley groove or insufficient friction, the transport process fails, and the lifting device is unable to perform its function. The purpose of the article and of the created measuring devices is to obtain by experimental measurements the most accurate true value possible of the coefficient of friction acting on the contact surface of the cable with the pulley groove. The values of the friction coefficients obtained by indirect measurements on laboratory equipment when the tractive force is transferred by friction differ in many cases and do not coincide with the values calculated using theoretical relationships. The aim of the paper is to present a method of measurement and to identify the magnitude of the forces acting on both sides of a cable belted in the V-groove of a cable drum. From the results obtained from the experimental measurements, to express the value of the random variable is based on the knowledge of the known values obtained from the measurements for their use in a failure analysis. This paper presents results that can be applied in the field of online monitoring of this type of lifting equipment for failure analysis, prediction and evaluation of their operational indicators.

Keywords: pulley; cable groove; friction coefficient; frictional force transfer; indirect measurement method; laboratory equipment

Citation: Hrabovský, L.; Fries, J.; Kudrna, L.; Gaszek, J. Determination of the Coefficient of Friction in a Pulley Groove by the Indirect Method. *Coatings* **2022**, *12*, 606. https://doi.org/10.3390/coatings12050606

Academic Editor: Lei Guo

Received: 12 April 2022
Accepted: 26 April 2022
Published: 29 April 2022

1. Introduction

In technical practice, fibre friction occurs, for example, in belt transmissions with V-belts and flat belts, cable transmissions (elevators, cable cars, ski lifts), conveyor belts, belt brakes, winches, etc. Fibre (also called belt) friction is the resistance that is imposed on a fibre (cable, conveyor belt, belt) as it slides over a curved surface. It is the friction of flexible fibres (ropes, straps and belts) on stationary and rotating cylindrical surfaces (rollers, pulleys, drums, discs).

In lifting devices, to improve the transmission capability and increase the traction capacity, the pulley's circumference has specially shaped grooves (V-shaped, semi-circular or semi-circular with a notch). The magnitude of the coefficient of shear friction in a pulley groove f_i [-] depends on the type of the groove and on the coefficient of shear friction μ [-] on the contact surfaces of the cable with the friction disc.

The measured values for the friction coefficient of the lining of a semi-circular groove in the friction disc of a mining machine with a friction disc (mine hoisting KOEPPE system) are given, for example, in [1]. In [1], Krešák et al. present the measured values of the friction

coefficient of rubber friction lining samples, which were compared with the values of the friction coefficient of the friction lining (K25) usually mounted on the friction lining pulley.

Dynamic force transfer by friction and slip between a steel cable and a friction disc groove lining during underground mining is discussed by Wang et al. in [2].

In the study [3], the dynamic contact characteristics between the mining cable and the friction lining of the semi-circular pulley groove in a deep mine were analysed by Wang. The evolution of the slip states and stress distribution along the bottom of the friction lining groove during load lifting and the influence of the friction coefficient on this evolution were investigated by Wang in [3] using the Finite Element Method.

In [4], Stawowiak et al. deal with the problem of friction between the cable and friction liner of a mining hoist.

Ge [5] investigated the frictional forces between a cable and the PVC groove lining and obtained friction coefficients related to the slip rate and pressure. It has been shown that the coefficient of friction decreases with increasing velocity or pressure.

Kumar at al. presents and discusses in a research article [6] an experimental method to determine the coefficient of friction when using the technique of friction stir welding.

Newly found evidence on the negative slope of the friction–velocity curve is described by Kim et al. [7] in terms of the contact area on the surface of brake friction materials. The tribotests were performed using two commercial friction materials with and without steel fibres.

Several studies have addressed the contact between the cable and the pulley [8], and others are based on physical experiments [9–11] rather than numerical simulations [12,13].

Hrabovsky [14] describes the design and implementation of a device on which it is possible to determine in the laboratory the friction coefficient value of a cable in given types of traction disc grooves.

Takehara et al. in [15] confirmed that the behaviour of a steel cable changes when both the modulus of elasticity of the steel cable in bending and the mass added to each end of the steel cable changes. Using numerical simulations, we confirm the proposed model of contact between the steel cable and the pulley.

The results obtained by Zhang in [16] show that the friction coefficient first decreases and then increases as the tension force increases and decreases linearly with an increasing cable speed. The effect of the cable speed on the temperature of the steel cable is greater than the effect of the tension force.

The testing of the rheological properties of friction-enhancing lubricant and the monitoring of temperature and friction coefficient changes during the friction process between a friction lining and steel cable are addressed in [17] by Feng et al.

The authors Ma and Lubrecht [18] studied the contact pressure between a steel cable and a friction block. The results from the numerical contact model show that the local maximum contact pressure is approximately 45 times greater than the average pressure obtained from the "planar method" formula.

Special technical applications where pulleys are used to transfer the tractive force by friction to a steel cable and to set a cleaning robot or a railway carriage in motion are dealt with in [19,20].

The dependence of the coefficients of friction and wear on the temperature of the materials of a friction pair, i.e., brake lining, is presented by Nosko, A. L et al. in [21].

Popper, D. and Weissenborn, H. [22] proposed a testing device for which the friction coefficients can be determined with greater accuracy than those defined by Coulomb's friction law and the Eytelwein equation [14].

Chang et al., studied the wear and friction characteristics of the steel wire rope and the evolution of the tribological parameters at different friction stages [23].

The results obtained by Yu-xing et al. [24] show that the coefficient of friction in the steady-state period changes very little with an increase in the contact load and that it stabilises at about 0.61.

Huang at al., in their paper [25], also discuss the development of the field of tribology, and highlight some of the main problems encountered in this area, such as the lack of systematicness, loose correlation, and inadequate focus on the microscopic perspective. In their article, they provide basic formulas of friction mechanics, taking into account friction's effect on the formulas of classical mechanics.

The study by Liu et al. [26] aims to find out the calculation formula for the friction resistance of steel wire's flexible shaft in the bending push-pull state. The operation principle is based on the adhesive friction theory and Newton's classical friction formula.

Guo et al. present in [27] a new theory of "global dynamic wrap angle" for friction hoists. The theory is based on a mine hoist simulation model which combines the suspended rope with the wrapped rope.

To calculate the pulling forces in the sides of a cable belted over a pulley, the Euler (Eytelwein) equation for fibre friction applies. By modifying the Euler equation, the coefficient of shear friction in a pulley groove can be expressed according to Equation (1).

$$f_i = \frac{1}{\alpha} \cdot \ln\left(\frac{F_n}{F_o}\right) \text{ [-]}, \tag{1}$$

In expression (1), α [rad] use is made of the belting angle in the arc measure, F_n [N] is the cable tension in the cable on the advancing part of the cable on the friction disc, F_o [N] is the cable tension on the retreating side.

2. Coefficient of Friction in a Pulley Groove

The magnitude of the shear friction coefficient in a pulley groove f_i depends on the type of groove (semi-circular, semi-circular with notch or V-groove) and the shear friction coefficient μ [-] on the contact surfaces of the cable with the pulley. The shear friction coefficient μ decreases with increasing contact pressure between the cable and the pulley [28] and is also affected by weather conditions.

According to ([28] chap. M.2.2), which was terminated on 6/2010, the friction coefficient for a V-groove can be expressed according to Equation (2), and for a semi-circular groove or a semi-circular groove with a notch according to Equation (3).

$$f = \frac{\mu}{\sin\left(\frac{\gamma}{2}\right)} \text{ [-]}, \tag{2}$$

$$f = \frac{4 \cdot \mu \cdot \left(1 - \sin\left(\frac{\beta}{2}\right)\right)}{\pi - \beta - \sin(\beta)} \text{ [-]}, \tag{3}$$

where β [rad]-the angle of the undercut of the groove or semi-circular groove ($\beta = 0$ for semi-circular groove), γ [rad]-the angle of the V-groove, $\mu = 0.09$-the coefficient of friction between the steel cable and the cast iron friction disc.

In [29], Janovský states that the traction capacity increases with a decreasing angle of the V-groove γ, but at the same time, the contact pressure on the contact area between the cable and the groove wall increases. The angle γ must therefore not be less than 32 deg, and it is recommended to choose $\gamma = 35 \div 40$ deg. In ([30] p. 23), it is stated that the β angle must not be greater than 105 deg, and a choice of up to 90 deg is recommended.

According to ([29] chap. M.2.2), which was terminated on 8/2017, the friction coefficient for a semi-circular groove or a semi-circular groove with a notch can be determined according to Equation (4), for V-groove not hardened according to Equation (3) and for hardened V-groove according to Equation (2).

$$f = \mu \cdot \frac{4 \cdot \left(\cos\left(\frac{\gamma}{2}\right) - \sin\left(\frac{\beta}{2}\right)\right)}{\pi - \beta - \gamma - \sin(\beta) + \sin(\gamma)} \text{ [-]}, \tag{4}$$

where β [deg]-the angle of the notch, γ [rad]-the angle of the V-groove (the value of γ suitable for the type of groove should be specified by the manufacturer. In no case should it be less than γ = 25 deg for a semi-circular groove. For a V-groove, it must not be less than γ = 35 deg), μ = 0.1-the coefficient of friction.

In Ref. ([31] pp. 43–44) and Ref. [32], it is stated that the maximum value of the notch angle β = 105 deg, should be chosen. The maximum size of the notch angle β_M = 106.3 deg (5) defines the width B [m] of the slot notch, which corresponds to 0.8 times the cable diameter d_L [m].

$$\sin\left(\frac{\beta_M}{2}\right) = \frac{B\ (= 0.8 \cdot d_L)}{d_L} \Rightarrow \beta_M = 2 \cdot \text{asin}(0.8)\ [\text{deg}], \quad (5)$$

The length of contact of a cable with the surface of a semi-circular groove can be expressed by $L_L = \delta \cdot d_L/2$ [m], where $\delta = \pi - \gamma$ [rad] is the angle of contact of the cable with the groove (see Figure 1). If the length of the contact between the cable and the surface of the semi-circular groove after the groove is formed is 20% of the length L_L [m], this length can be expressed as $L_{Ld} = 0.2 \cdot L_L$ [m]. The maximum size of the notch angle can be determined by the expression $\beta_{max} = 2 \cdot (L_L - L_{Ld})/d_L$ [deg].

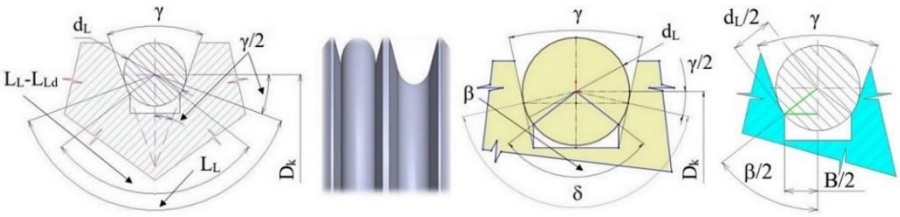

Figure 1. Cable of circular cross-section running through a semi-circular groove with a notch.

Table 1 shows the values of the friction coefficient in the semi-circular (according to Equation (4)) groove and V-groove (according to Equations (2) and (3)) of the pulley for the V-groove angle γ = 35 ÷ 40 deg (for β = 0 deg).

Table 1. Coefficient of friction in the pulley groove.

γ	[deg]	35	36	37	38	39	40
f (2)		0.3326	0.3236	0.3152	0.3072	0.2996	0.2924
f (3)	[-]				0.1273		
f (4)		0.1229	0.1227	0.1225	0.1222	0.1220	0.1218

The calculated values of the advancing force F_n on the pulley induced by the magnitude of the retreating force F_o in the semi-circular groove according to Equation (4), and in the hardened V-groove according to Equation (2), for the V-groove angle γ = 40 deg are given in Table 2.

Table 2. Pulling forces in the sides of a cable belted around a pulley.

m_z	F_n	γ_1	f *1	e·exp(f·α)	F_o	γ_{21}	f *2	e·exp(f·α)	F_o
[kg]	[N]	[deg]	[-]	-	[N]	[deg]	[-]	-	[N]
5	49.03				33.44				17.25
10	98.07				66.89				34.50
15	147.10				100.33				51.72
20	196.13	40	0.122	1.466	133.78	35	0.333	2.843	69.00
25	245.17				167.22				86.25
30	294.20				200.67				103.49
35	343.23				234.11				120.74

*1 see Equation (4), *2 see Equation (2).

3. Experimental Determination of the Coefficient of Friction of a Cable in a Pulley V-Groove

3.1. Description of the Experimental Apparatus and Method of Detecting the Pulling Force in the Cable

In the V-groove (V-groove angle γ = 35 deg) of the three-groove pulley 2 with a pitch diameter D = 740 mm, a steel cable 1 with a nominal diameter d_L = 8 (or 10) mm was belted, and a load 3 with a gravity G [N] was successively suspended from its free end on the left side of the pulley (see Figure 2). The belting angle α = 180 deg of the cable in the V-groove of the pulley defines the magnitude of contact, i.e., the length of the arc over which the cable is in contact with the pulley groove.

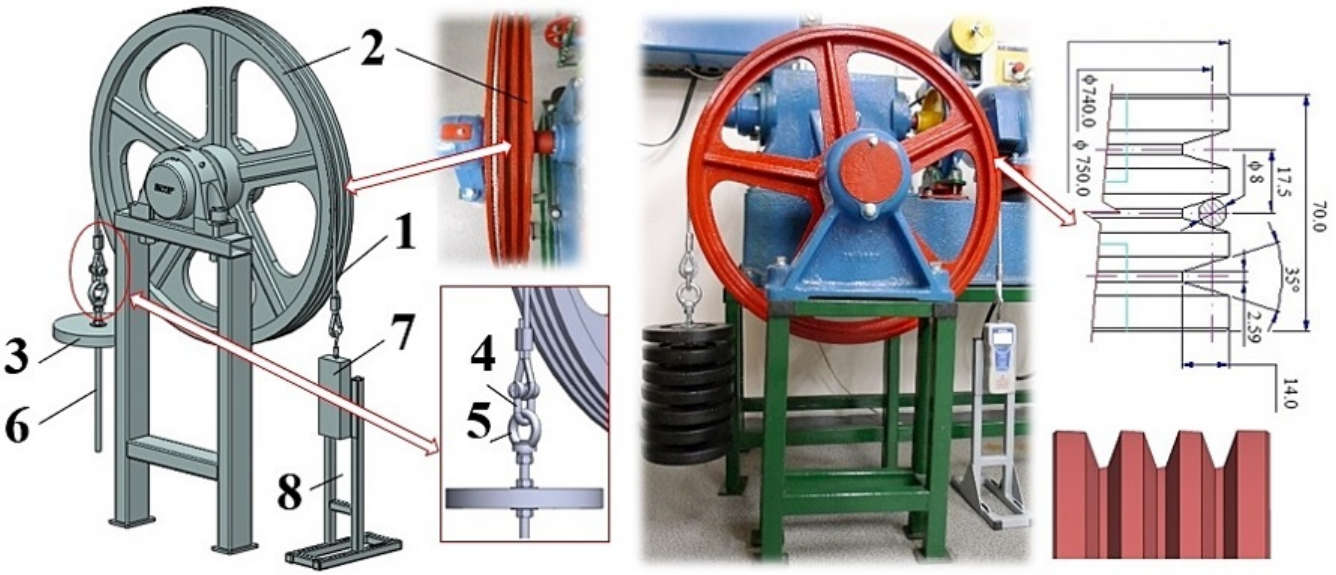

Figure 2. Experimental apparatus used to determine the coefficient of friction in the pulley V-groove.

Fork 4 (according to DIN 82101—FORM A) is screwed onto the loop with eyelet thimble (according to DIN 3090) of one of the ends of the steel cable 1 (design 6x19-FC, wire strength min. 1770 MPa), length 1.6 m, clamped with sleeves (according to EN 13411-3). An eye nut 5 (according to DIN 582) is put on the fork 4. A threaded rod 6 with a length of 350 mm is screwed onto the internal thread of the M12 nut 5. The threaded rod 6 is prevented from unscrewing from the nut 5 by a spring washer, washer and hex nut. Between the nuts and washers, there are 3 weights (weight of one piece, m_z = 5 kg).

The loop with eyelet thimble (according to DIN 3090) of the other end of the steel cable 1 is suspended from the hook of a force gauge 7, which is mechanically bolted to the welded structure 8. The supporting structure 8 is anchored to the laboratory floor with bolts.

3.2. Laboratory-Determined Values of Static Forces in Cables Running across Pulley V-Groove

The values of the acting forces F_{oMi} [N] on the retreating (right) side of the pulley obtained by laboratory measurements on an experimental device (Figure 2) were obtained for two cable types (cable diameter 8 mm and 10 mm) and under two operating conditions that define the surface of the V-groove: a) dry and clean, b) contaminated with oil.

The magnitudes of the forces measured by the F_{oMi} force gauge 7 were generated by gradually increasing the weight G 3 suspended from the cable 1 on the advancing (left) side of the pulley 2.

The value of the friction coefficient f_{Mi} [-] cannot be measured directly on the experimental device (Figure 2), so the sought-after friction coefficient f_{Mi} (see Table 3) had to be calculated from the mathematically modified Euler equation (see relation (1)) assuming known values of F_n, F_o and α. The cable was belted in the pulley groove at an angle α = 180 deg, the magnitude of the advancing force F_{ni} was chosen as the weight G_i (given by the number of i weight of one piece, m_z) suspended on the cable on the left side of the

pulley (Figure 2), and the magnitude of the retreating force F_{oMi} was obtained by reading from a force gauge 7.

Table 3. Friction coefficient, dry groove, 10 mm diameter cable.

m_z	F_N	F_{oM1}	f_{M1}	F_{oM2}	f_{M2}	F_{oM3}	f_{M3}	F_{oM4}	f_{M4}	F_{oM5}	f_{M5}	$f_{Mi} \pm \kappa_{a,n}$ *3
[kg]	[N]		[-]	[N]	[-]	[N]	[-]	[N]	[-]	[N]	[-]	-
5	49.03	14	0.399	13	0.423	15	0.377	15	0.377	14	0.399	0.395 ± 0.024
10	98.07	26	0.423	28	0.399	27	0.411	26	0.423	27	0.411	0.413 ± 0.012
15	147.10	39	0.423	38	0.431	37	0.439	38	0.431	37	0.439	0.433 ± 0.008
20	196.13	54	0.411	53	0.417	54	0.411	53	0.417	53	0.417	0.415 ± 0.004
25	245.17	68	0.408	69	0.404	69	0.404	68	0.408	68	0.408	0.406 ± 0.003
30	294.20	82	0.407	83	0.403	83	0.403	82	0.407	83	0.403	0.405 ± 0.003
35	343.23	95	0.409	94	0.412	95	0.409	93	0.416	94	0.412	0.412 ± 0.004
The average value of the measured values of *f*												0.411

*3 f_{Mi}—arithmetic mean of all f_{Mi}, $\kappa_{a,n}$ values—extreme measurement error, for risk "a" and "n" measurements.

From Figure 3 it is seen that the highest measured value of the friction coefficient in the V-groove (γ = 35 deg) of the pulley is f_{max} = 0.441, which expresses a value 32.4% higher than the value of the friction coefficient (f = 0.333) expressed according to relation (2). From Figure 3 it is also seen that the lowest measured value of the coefficient of friction in the V-groove (γ = 35 deg) of the pulley is f_{min} = 0.371, which expresses a value 11.4% higher than the coefficient of friction f calculated according to relation (2).

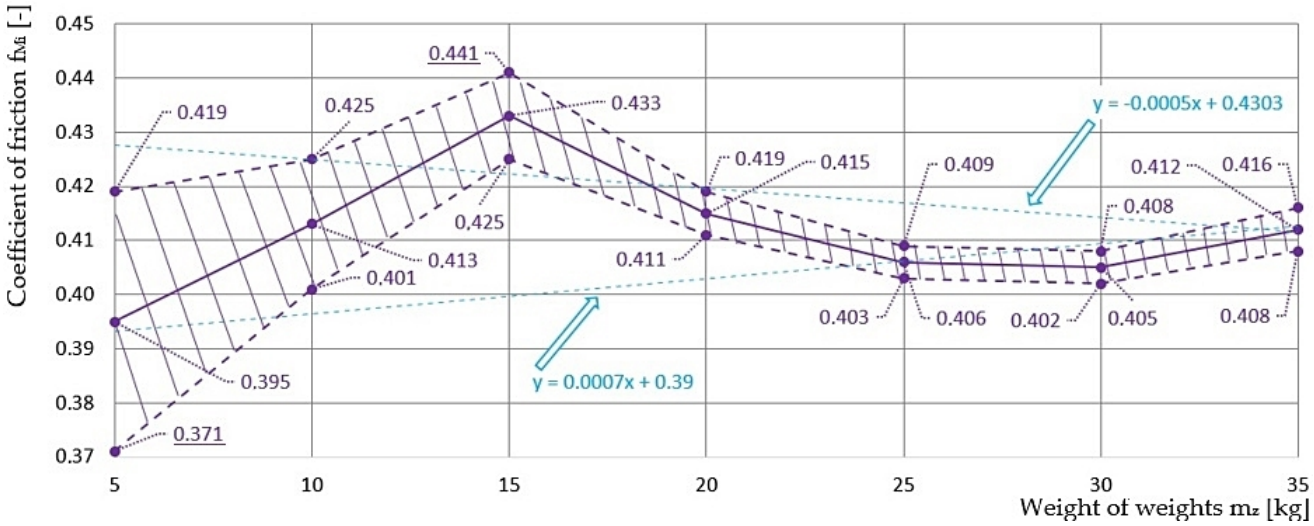

Figure 3. Experimentally determined friction coefficient values, 8 mm diameter cable, dry and clean groove surface.

Measured values of friction coefficient f_{Mi} for dry groove and 8 mm diameter cable are given in Table 4.

Table 4. Friction coefficient, dry groove, 8 mm diameter cable.

m_z	F_N	F_{oM1}	f_{M1}	F_{oM2}	f_{M2}	F_{oM3}	f_{M3}	F_{oM4}	f_{M4}	F_{oM5}	f_{M5}	$f_{Mi} \pm \kappa_{a,n}$ *3
[kg]	[N]		[-]	[N]	[-]	[N]	[-]	[N]	[-]	[N]	[-]	-
5	49.03	13	0.423	14	0.399	14	0.399	13	0.423	13	0.423	0.413 ± 0.016
10	98.07	25	0.435	27	0.411	25	0.435	26	0.423	26	0.423	0.425 ± 0.012
15	147.10	37	0.439	38	0.431	38	0.431	37	0.439	38	0.431	0.434 ± 0.005
20	196.13	51	0.429	50	0.411	53	0.417	54	0.411	54	0.411	0.416 ± 0.010
25	245.17	69	0.404	68	0.408	68	0.408	68	0.408	68	0.408	0.407 ± 0.002
30	294.20	83	0.403	82	0.407	83	0.403	82	0.407	82	0.407	0.405 ± 0.003
The average value of the measured values of *f*												0.417

*3 see Table 3.

From Figure 4 it is seen that the highest measured value of the friction coefficient in the V-groove (γ = 35 deg) of the pulley is f_{max} = 0.439, which expresses a value 31.8% higher than the value of the friction coefficient f expressed according to relation (2).

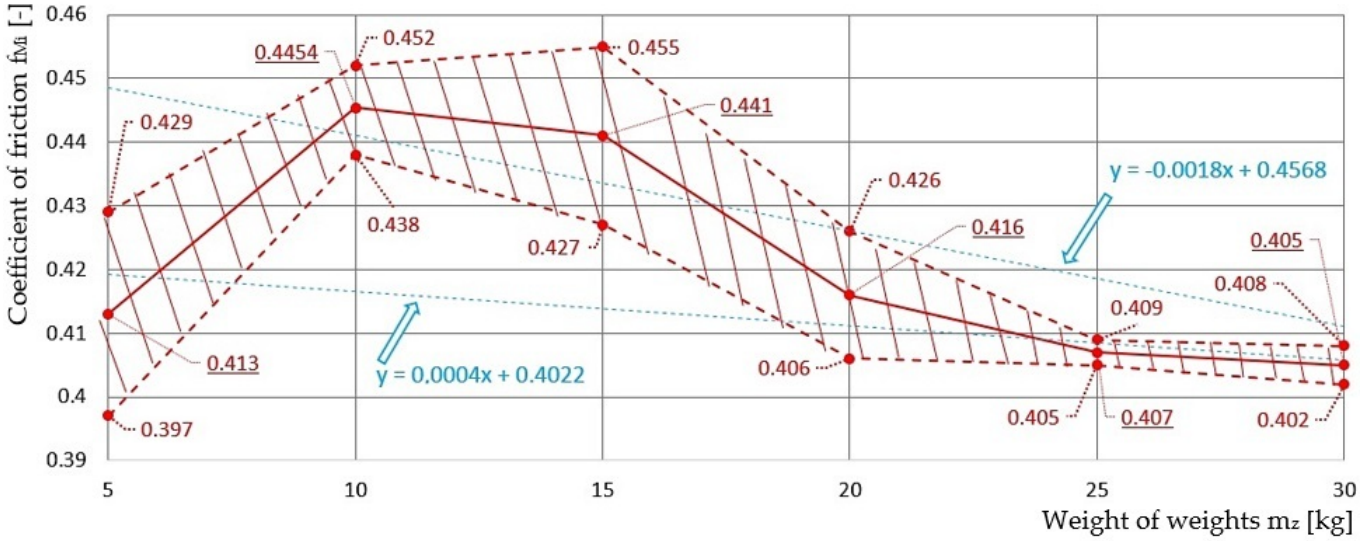

Figure 4. Friction coefficient values obtained by laboratory measurement, 8 mm diameter cable, groove surface contaminated with oil.

From Figure 4, it is also seen that the lowest measured value of the friction coefficient in the V-groove (γ = 35 deg) of the pulley is f_{min} = 0.397, which expresses a value 19.2% higher than the friction coefficient f (2).

Measured values of friction coefficient f_{Mi} for groove contaminated with oil and 10 mm diameter cable are given in Table 5 and Figure 5.

Table 5. Coefficient of friction, groove contaminated with oil, 10 mm diameter cable.

m_z	F_N	F_{oM1}	f_{M1}	F_{oM2}	f_{M2}	F_{oM3}	f_{M3}	F_{oM4}	f_{M4}	F_{oM5}	f_{M5}	$f_{Mi} \pm \kappa_{a,n}$ *3
[kg]	[N]		[-]	[N]	[-]	[N]	[-]	[N]	[-]	[N]	[-]	-
5	49.03	18	0.319	17	0.337	18	0.319	19	0.302	18	0.319	0.319 ± 0.015
10	98.07	31	0.367	33	0.347	35	0.328	34	0.337	33	0.347	0.345 ± 0.018
15	147.10	44	0.384	46	0.370	47	0.363	46	0.370	45	0.377	0.373 ± 0.010
20	196.13	56	0.399	54	0.411	58	0.388	55	0.405	57	0.393	0.399 ± 0.011
25	245.17	70	0.399	72	0.390	71	0.394	71	0.394	70	0.399	0.395 ± 0.005
30	294.20	86	0.391	85	0.395	87	0.388	86	0.391	85	0.395	0.392 ± 0.004
The average value of the measured values of *f*												0.371

*3 see Table 3.

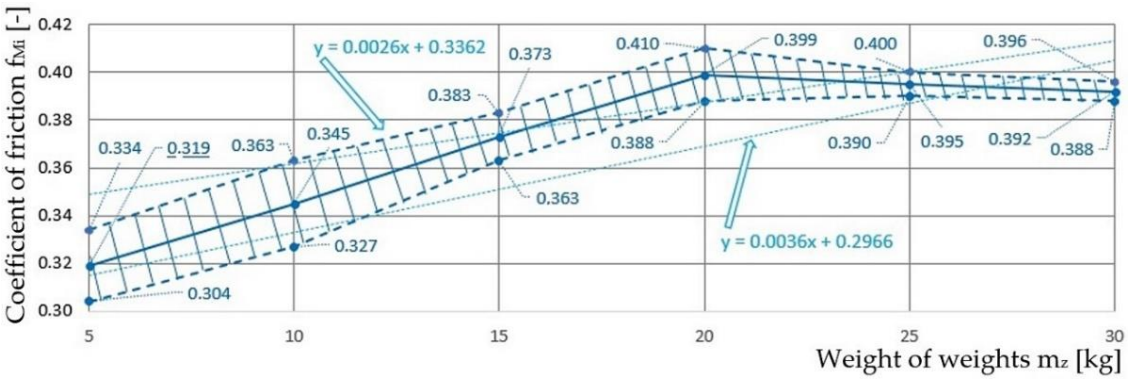

Figure 5. Values of the friction coefficient obtained in the laboratory, 10 mm diameter cable, dry and clean groove surface.

Measured values of friction coefficient f_{Mi} for groove contaminated with oil and 8 mm diameter cable are given in Table 6.

Table 6. Coefficient of friction, groove contaminated with oil, 8 mm diameter cable.

m_z	F_N	F_{oM1}	f_{M1}	F_{oM2}	f_{M2}	F_{oM3}	f_{M3}	F_{oM4}	f_{M4}	F_{oM5}	f_{M5}	$f_{Mi} \pm \kappa_{a,n}$ *3
[kg]	[N]		[-]	[N]	[-]	[N]	[-]	[N]	[-]	[N]	[-]	-
5	49.03	17	0.337	16	0.356	15	0.377	16	0.356	17	0.337	0.353 ± 0.021
10	98.07	38	0.302	36	0.319	38	0.302	36	0.319	37	0.310	0.310 ± 0.011
15	147.10	51	0.337	50	0.343	49	0.350	50	0.343	49	0.350	0.345 ± 0.007
20	196.13	66	0.347	65	0.352	64	0.356	65	0.352	66	0.347	0.351 ± 0.005
25	245.17	74	0.381	76	0.373	76	0.373	75	0.377	74	0.381	0.377 ± 0.005
30	294.20	85	0.395	86	0.391	86	0.391	85	0.395	86	0.391	0.396 ± 0.003
The average value of the measured values of *f*												0.355

*3 see Table 3.

3.3. Experimental Station Designed to Detect Forces in Pulley Cable

The magnitude of the transmitted circumferential force F [N] (Equation (6)) from the drive to the cable by friction in the pulley groove depends on the belting angle α, the tension in the cable behind the pulley F_o and the coefficient of the shear friction in the pulley groove f_i.

$$F = F_N - F_o = F_o \cdot \left(e^{f_i \cdot \alpha} - 1\right) \text{ [N]}, \quad (6)$$

For indirect laboratory measurements of the friction coefficient f_i in the semi-circular and V-groove, a laboratory device was developed which consists of an electric gearbox 8 on the output shaft on which (diameter d = 28 mm) is mounted a pulley 2. The steel cable 1 with a final length (design 6x7-WSC, strength of wires min. 1960 MPa) and with a diameter of 6 mm or 8 mm runs through a groove (semi-circular γ = 40 deg or V-groove γ = 35 deg [33]) with a spacing diameter of D_k = 320 mm, created on the circumference of the cable pulley 2. Both ends of cable 1 are terminated with eyelets and clamped with clamps (according to EN 13411-3).

On the loop with the eyelet thimble (according to DIN 3090) of the steel cable 1 on the retreating (left) side of the pulley, the same parts are installed as in the experimental device (see Figure 2).

A shackle pin 4 (DIN 82101—FORM A) is threaded through the loop with the eyelet thimble (according to DIN 3090) of the other end of the steel cable 1 (the advancing side of the cable on the pulley), on which an eye bolt 7 (DIN 580) is mounted. An eye bolt 7 is screwed onto the internal thread M12 on the upper surface of the strain gauge load cell 9. An eye bolt 7 is also screwed into the M12 threaded hole in the bottom surface of the load cell 9, and a shackle 4 is slipped over its eye.

Measured values of friction coefficient f_{Mi} for groove contaminated with oil and 8 mm diameter cable are given in Figure 6.

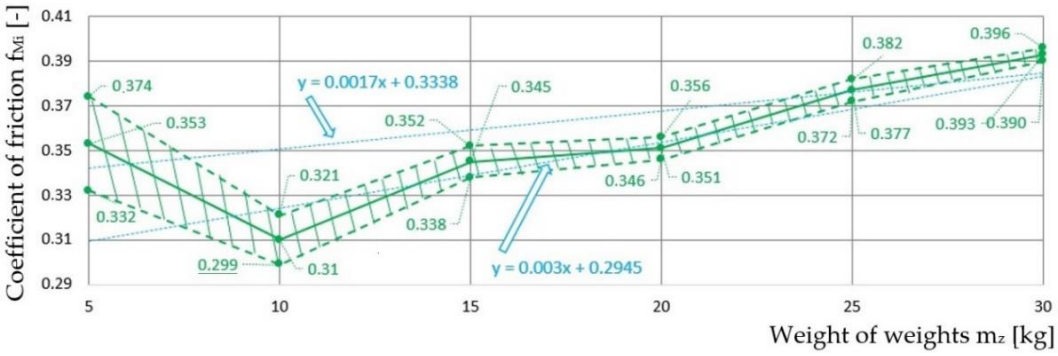

Figure 6. Laboratory-derived friction coefficient values for a 10-mm diameter cable and a groove surface contaminated with oil.

An eye bolt 7 is screwed onto the shackle pin 4, the threaded part of which is screwed onto the internal thread of the nut 10 (special design), which is inserted into a groove in the profile of the aluminum frame structure of the laboratory equipment (Figure 7).

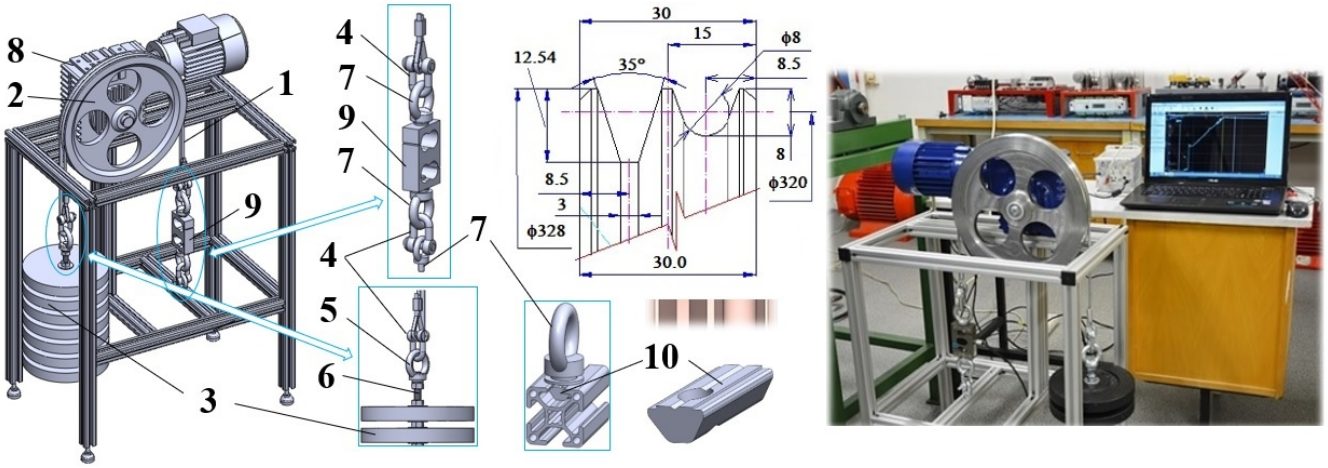

Figure 7. Laboratory equipment used to measure the pulling force on the advancing side of the cable on the pulley.

On the laboratory equipment (see Figure 7) the instantaneous magnitude of the F_N force is sensed by the load cell RSCC 9 [34] on the advancing side of the cable 1 on the pulley 2 under the action of the torque M_2 [N·m] on the shaft of the pulley 2, which is generated by the electro-gear transmission 8 [35].

Table 7 shows the theoretically calculated values of the pulling force F_N on the advancing side of the cable on the pulley according to the Euler equation for the angle γ = 40 deg of the semi-circular groove and the angle γ = 35 of the V-groove.

Table 7. Pulling forces in the sides of a cable running over a pulley groove for different groove angles.

m_z	F_o	γ_1	f *4	e·exp(f·α)	F_N	γ_{21}	f *5	e·exp(f·α)	F_N
[kg]	[N]	[deg]	[-]	-	[N]	[deg]	[-]	-	[N]
5	49.03				71.89				139.38
10	98.07				143.78				278.77
15	147.10				215.67				418.15
20	196.13	40	0.122	1.466	287.55	35	0.333	2.843	557.54
25	245.17				359.44				696.92
30	294.20				431.33				836.31
35	343.23				503.22				975.69

*4 see Equation (4), *5 see Equation (2).

Table 8 shows the theoretically calculated values of the pulling force F_N on the advancing side of the cable on the pulley according to the Euler equation for the angle γ = 37 and 40 deg of the V-groove.

The aim of the prepared experimental measurements is to verify the theoretically calculated values of the pulling force F_N with the laboratory measured values of the force F_{Nm} [N] on a laboratory device (Figure 7).

The values of the pulling forces on both sides of the cable (F_N and F_o) of the belting angle α = 180 deg of a pulley of pitch diameter D_k depending on the weight m_z and the V-groove angle γ are shown in Figure 8.

Table 8. Pulling forces in the sides of a cable running over a pulley groove for different groove angles.

m_z	F_o	γ_1	f *5	e·exp(f·α)	F_N	γ_{21}	f *5	e·exp(f·α)	F_N
[kg]	[N]	[deg]	[-]	-	[N]	[deg]	[-]	-	[N]
5	49.03				131.97				122.86
10	98.07				263.94				245.72
15	147.10				395.91				368.58
20	196.13	37	0.315	2.691	527.89	40	0.292	2.506	491.44
25	245.17				659.86				614.3
30	294.20				791.83				737.16
35	343.23				923.80				860.01

*5 viz (2).

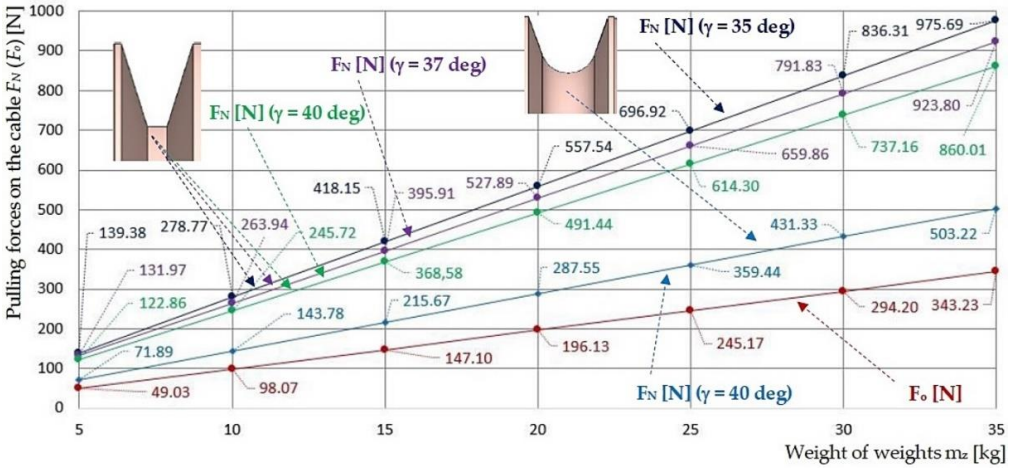

Figure 8. Pulling forces F_N and F_o on the cable on the advancing and retreating side of the pulley of the laboratory device.

The electro-transmission 8 consists of an electric motor (type 4AP71-4) with power P_e = 370 W and speed n_e = 1370 min^{-1} and a gearbox (type aC-63 ([35] p. 14)) with gear ratio i_p = 31.5.

4. Discussion

A weight 3 of known mass m_z is suspended from the end of cable 1 (on the retreating side of the pulley 2, see Figure 7). The derived pulling force F_N on the advancing side of the pulley 2 by the weight 3 is detected by the load cell RSCC 9. A load sensor cable 9 equipped with a D-Sub plug was plugged into the socket of the measuring module BR4-D of the strain gauge apparatus DS NET during the laboratory measurements. A PC (ASUS K72JR-TY131 laptop) was connected to the DS NET strain gauge using a network cable with RJ-45 connectors at both ends. The time record of the measured F_N pulling force was displayed on a PC screen in the DEWESoft X2 SP5 software environment (see Figure 9).

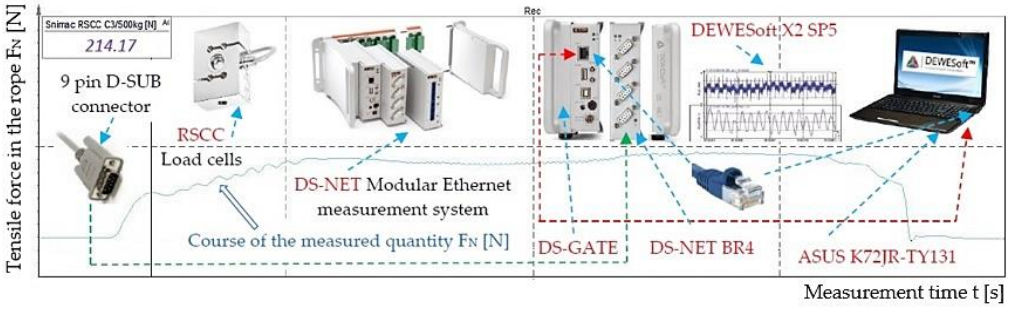

Figure 9. Time course of the measured tractive force F_N on the advancing side of the cable on the pulley of the laboratory device.

Through the supply of an electric current to the terminals of the electric motor, a tractive force F_2 [N] acts on the pitch diameter D_k of the pulley 2, which attempts to move the cable 1 in the pulley groove due to the frictional effect. Due to the anchoring of the cable 1 on the advancing side to the frame of the laboratory equipment (Figure 7), the frictional force F_T [N] is generated on the contact area of the cable with the pulley groove under the action of the torque M_2. The instantaneous magnitude of the friction force F_T can be expressed as the product of the normal force N [N] and the friction coefficient of the cable in the groove f. The normal force can be expressed as the sum of the instantaneous magnitudes of the pulling forces in both cable sides $N = F_o + F_N$.

When the tractive force is transmitted by friction, relation (6) applies to the circumferential force F. The magnitude of the pulling force F_N on the advancing side of the cable on the pulley increases with the increasing belting angle α of the cable through the pulley groove.

The pulling force F_N reaches the maximum value for the laboratory device (see Figure 7) at a belting angle α = 180 deg. If the drive supplies the tractive force F_2, and if the maximum possible size of the circumferential force in the pulley groove is F (6), at $F_2 > F$, the cable slips in the pulley groove. Figure 10 present the measured force waveform of F_N, using the RSCC 9 load cell on the laboratory equipment.

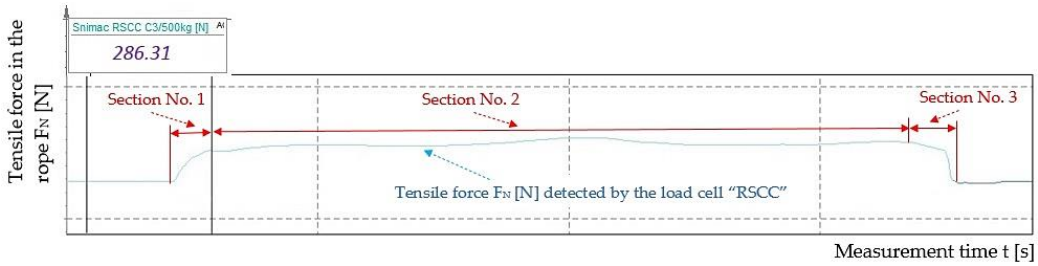

Figure 10. Pulling force waveform of F_N measured by RSCC load cell on laboratory equipment.

Experimental measurements of the generated pulling force in the cable were carried out on a measuring device (Figure 2) under the static condition of the pulley, i.e., the cable was not subjected to friction in the groove of the rotating pulley. The experimentally measured F_{oMi} forces listed in Tables 3–6 were detected by an IMADA force meter with a measuring range of 0 ÷ 1000 N, a resolution of 1 N and an accuracy of ±2%. The values of the friction coefficients in the V-groove f_{Mi} determined by the indirect method from the measurements carried out on the experimental device (see Figure 2) were calculated from relation (1). Refinement of the measured F_{oMi} force values could be achieved by using a force gauge with more sensitive resolution.

The laboratory results of the friction coefficients confirm the assumption that the coefficient of friction of the cable in the pulley groove reaches smaller values for the operating condition when the contact surfaces of the groove are contaminated with oil in relation to the operating condition of the groove dry and clean, see Figure 11.

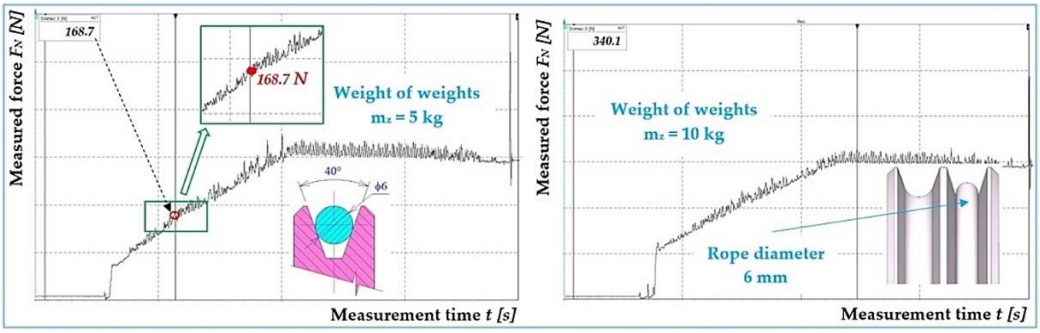

Figure 11. The force waveform of F_N measured by RSCC load cell on laboratory equipment.

The theoretical assumptions, see Figure 12, of the physical phenomenon known as fibre friction and the validity of the Euler equation for fibre friction were also confirmed by experimental measurements. The measured values of the coefficient of friction of the 10 mm diameter cable under the condition of the groove "dry and clean" showed values about 32% higher than the recommended value according to [36]. This difference between the measured and the actual value of the coefficient of friction of the cable in the hardened V-groove can be justified by the fact that the technical standard [30] gives a recommended value for the calculation which takes into account the least favourable operating condition of the contamination of the groove.

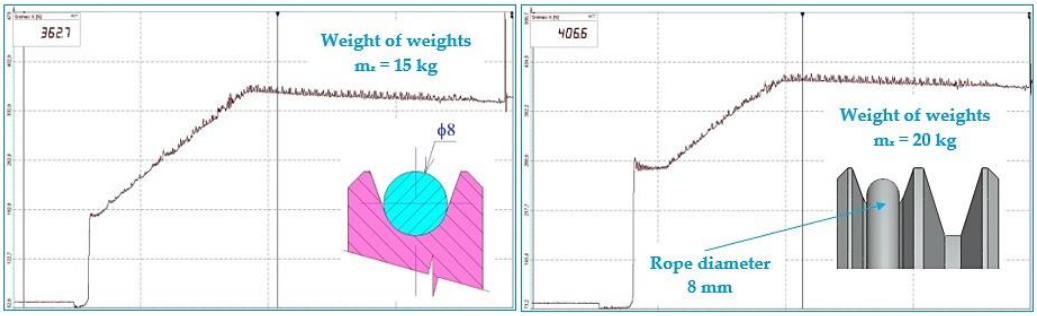

Figure 12. Pulling force F_N on the cable on the advancing side of the pulley of the laboratory device.

5. Conclusions

This paper presents two experimental devices designed at the Department of Machine and Industrial Design, Faculty of Mechanical Engineering, VSB-Technical University of Ostrava, and constructed in the Laboratory of Research and Testing. Both laboratory devices are used to detect pulling forces in both sides of the final length of a cable belted in a pulley groove and to verify the phenomenon defined by the name fibre friction.

The purpose of the created measuring devices (Figures 2 and 7) is to obtain by experimental measurements the most accurate true value possible of the coefficient of friction acting on the contact surface of the cable with the pulley groove. The values of the friction coefficients obtained by indirect measurements on laboratory equipment, when the tractive force is transferred by friction, differ in many cases and do not coincide with the values calculated using theoretical relationships, e.g., (2), (3) and (4).

A notch which can be formed in the base of the groove profile of the pulley can reduce the contact pressure on the contact area of the cable running through a semi-circular groove. The width of the groove must be designed in accordance with [30] so that its size reaches a maximum of 80% of the cable diameter. The relation (5) gives the maximum value that can be used for the angle of the groove.

The instantaneous value of the tractive force on the advancing cable side while the pulley was rotating was recorded during the time period of each measurement, while laboratory measurements were performed on the measuring device (Figure 7). The plotted time history of the F_N tractive force on the laboratory device (see Figure 10), is composed of three basic parts.

The first section of the time record of the measured F_N force is defined by a rising curve. This section presents the increase in the magnitude of the tractive force F_N on the advancing side of the cable on the driven pulley. When the pulley rotates, the tractive force F_N increases according to Euler's equation for fibre friction to its maximum value, which is defined by the friction factor (the size of the cable girth angle α and the friction coefficient f in the pulley groove). If the magnitude of the force in the cable reaches the maximum value of the circumferential force F (given by the difference between F_N and tractive force F_o on the retreating side of the cable from the pulley, which is equal to the weight suspended from the end of the cable, at the belting angle α), which is greater than the frictional force F_T of the loaded cable, the cable will start to slip in the pulley groove (assuming a sufficient magnitude of the tractive force F_2 and torque M_2).

The second section of the time record of the measured force F_N is defined by a horizontal curve and presents the slip of the cable in the pulley groove.

The third section of the time record of the measured F_N force is defined by a falling curve. When the power supply to the electric motor terminals is interrupted, the pulling force F_2 ceases to act on the pitch diameter D_k of the pulley. The maximum magnitude of the measured force F_N drops to a value equal to the magnitude of the tractive force on the retreating side, i.e., to the value F_o.

By successive (repeated under the same conditions) laboratory measurements of the tractive force F_N (Figures 11 and 12) on the advancing side of the cable on the pulley at a known belting angle α = 180 deg, it is possible to determine on laboratory equipment (Figure 7) by the indirect method the actual value of the coefficient of friction in a given type of cable groove (semi-circular, V-groove) under the operating conditions of surface contamination (clean and dry, contaminated with dust, contaminated with oil, etc.) of the groove surfaces in contact with the steel cable. The actual value of the friction coefficient obtained by laboratory measurement can be verified with the values theoretically calculated (see Table 7) according to relations (2) to (4).

Author Contributions: Conceptualisation, L.H. and J.F.; methodology, software, L.H. and L.K.; validation, L.H., J.F. and J.G.; formal analysis, investigation, resources, data curation, writing-original draft preparation, writing-review and editing and visualisation, L.H., J.F. and L.K.; supervision, project administration and funding acquisition, J.F. and J.G. All authors have read and agreed to the published version of the manuscript.

Funding: This research was funded by The Ministry of Education, Youth and Sports of The Czech Republic, Grant No. SP2022/2 and Ministry of Industry and Trade of the Czech Republic was funded by EG20_321/0024559.

Institutional Review Board Statement: Not applicable.

Informed Consent Statement: Not applicable.

Data Availability Statement: The authors confirm that the data supporting the findings of this study are available within the article.

Acknowledgments: This work has been supported by The Ministry of Education, Youth and Sports of the Czech Republic from the Specific Research Project SV3402256 (SP2022/2) and Ministry of Industry and Trade of the Czech Republic from the Specific Research Project EG20_321/0024559 (MP342132).

Conflicts of Interest: The authors declare no conflict of interest.

References

1. Kresak, J.; Peterka, P.; Ambrisko, L.; Mantic, M. Friction lining coefficient of the drive friction pulley. *Eksploat. Niezawodn.* **2021**, *23*, 338–345. [CrossRef]
2. Wang, D.; Zhang, D.; Mao, X.; Peng, Y.; Ge, S. Dynamic friction transmission and creep characteristics between hoisting rope and friction lining. *Eng. Fail. Anal.* **2015**, *57*, 499–510. [CrossRef]
3. Wang, D. Dynamic contact characteristics between hoisting rope and friction lining in the deep coal mine. *Eng. Fail. Anal.* **2016**, *64*, 44–57. [CrossRef]
4. Stawowiak, M.; Zołnierz, M. Mobile test stand validation for measuring friction coefficient of carrying rope with friction lining. *Manag. Syst. Prod. Eng.* **2018**, *26*, 143–150. [CrossRef]
5. Ge, S. The friction coefficients between the steel rope and polymer lining in frictional hoisting. *Wear* **1992**, *152*, 21–29. [CrossRef]
6. Kumar, K.; Kalyan, C.; Kailas, S.V.; Srivatsan, T.S. An investigation of friction during friction stir welding of metallic materials. *Mater. Manuf. Process.* **2009**, *24*, 438–445. [CrossRef]
7. Kim, J.W.; Joo, B.S.; Jang, H. The effect of contact area on velocity weakening of the friction coefficient and friction instability: A case study on brake friction materials. *Tribol. Int.* **2019**, *135*, 38–45. [CrossRef]
8. Klaus, F. *Wire Ropes*; Springer: Berlin, Germany, 2007; pp. 194–195.
9. Shabana, A.A. Finite element incremental approach and exact rigid body inertia. *J. Mech. Des.* **1996**, *118*, 171–178. [CrossRef]
10. Takehara, S.; Kawarada, M.; Hase, K. Dynamic contact between a wire rope and a pulley using absolute nodal coordinate formulation. *Machine* **2016**, *4*, 4. [CrossRef]

11. Zhang, J.; Wang, D.; Song, D.; Zhang, D.; Zhang, C.; Araujo, J.A. Tribo-fatigue behaviors of steel wire rope under bending fatigue with the variable tension. *Wear* **2019**, *428*, 154–161. [CrossRef]
12. Imanishi, E.; Nanjo, T.; Kobayashi, T. Dynamic simulation of wire rope with contact. *J. Mech. Sci. Technol.* **2009**, *23*, 1083–1088. [CrossRef]
13. Lugris, U.; Escalona, J.L.; Dopico, D.; Cuadrado, J. Efficient and accurate simulation of the rope–sheave interaction in weight-lifting machines. *Proc. Inst. Mech. Eng. Part K J. Multi-Body Dyn.* **2011**, *225*, 331–343. [CrossRef]
14. Hrabovsky, L.; Michalik, P. Friction Coefficient of Load-Bearing Elements of Building Technical Facilities. In *IOP Conference Series: Materials Science and Engineering*; IOP Publishing Ltd.: Bristol, UK, 2021; p. 1203.
15. Blau, P.J. The significance and use of the friction coefficient. *Tribol. Int.* **2001**, *34*, 585–591. [CrossRef]
16. Zhang, Q.; Peng, Y.; Zhu, Z.; Tang, W.; Chen, G.; Zhao, X.; Wang, F. Studies on friction and wear characteristics of wire rope used in multi-layer winding hoist during inter-circle transition under dry friction. *Proc. Inst. Mech. Eng. Part J J. Eng. Tribol.* **2022**, *236*, 90–104. [CrossRef]
17. Feng, C.; Zhang, D.; Chen, K.; Guo, Y. Study on viscoelastic friction and wear between friction linings and wire rope. *Int. J. Mech. Sci.* **2018**, *142*, 140–152. [CrossRef]
18. Ma, W.; Lubrecht, A.A. Detailed contact pressure between wire rope and friction lining. *Tribol. Int.* **2017**, *109*, 238–245. [CrossRef]
19. Malakova, S.; Sivak, S.; Harachova, D.; Mantic, M.; Kulka, J. Design of gearbox lubrication system. *GRANT J.* **2021**, *10*, 90–93.
20. Hrabovsky, L.; Mantic, M.; Vostova, V. Adhesion coefficient on the limit of slippage at star-up of the manual crane trolley. *Adv. Sci. Technol. Res. J.* **2019**, *13*, 92–99. [CrossRef]
21. Nosko, A.L.; Safronov, E.V.; Soloviev, V.A. Study of friction and wear characteristics of the friction pair of centrifugal brake rollers. *J. Frict. Wear* **2018**, *39*, 145–151. [CrossRef]
22. Popper, D.; Weissenborn, H. Friction coefficient between the rope and the drive pulley of Koepe winders. *Neue Bergbautech.* **1982**, *12*, 271–273.
23. Chang, X.D.; Peng, Y.X.; Zhu, Z.C.; Zou, S.Y.; Gong, X.S.; Xu, C.M. Evolution Properties of Tribological Parameters for Steel Wire Rope under Sliding Contact Conditions. *Metals* **2018**, *8*, 743. [CrossRef]
24. Peng, Y.-X.; Chang, X.-D.; Zhu, Z.-C.; Wang, D.-G.; Gong, X.-S.; Zou, S.-Y.; Sun, S.-S.; Xu, W.-X. Sliding friction and wear behavior of winding hoisting rope in ultra-deep coal mine under different conditions. *Wear* **2016**, *368*, 423–434.
25. Huang, P.; Yang, Q. Theory and contents of frictional mechanics. *Friction* **2014**, *2*, 27–39. [CrossRef]
26. Liu, Y.; Li, J.; Wang, T.; Ding, Y.; Wang, G. Study on the friction resistance calculation method of a flexible shaft of wire rope based on genetic algorithm. *Mech. Adv. Mater. Struct.* **2021**, 1–15. [CrossRef]
27. Guo, Y.; Zhang, D.; Zhang, X.; Wang, D.; Wang, S. A New Transmission Theory of Global Dynamic Wrap Angle for Friction Hoist Combining Suspended and Wrapped Wire Rope. *Appl. Sci.* **2020**, *10*, 1305. [CrossRef]
28. *ČSN EN 81-1*; Bezpečnostní Předpisy pro Konstrukci a Montáž Osobních a Nákladních a Malých Nákladních Výtahů. Část 1: Elektrické Výtahy (In English: Safety Rules for the Construction and Instalation of Lifts-Part 1: Electric Lifts). ČNI: Praha, Czech Republic, 1994; p. 92.
29. *ČSN EN 81-1+A3*; Bezpečnostní Předpisy pro Konstrukci a Montáž Výtahů-Část 1: Elektrické Výtahy (In English: Safety Rules for the Construction and Installation of Lifts-Part 1: Electric Lifts). ČNI: Praha, Czech Republic, 2010; p. 92.
30. Janovsky, L. *Systémy a Strojní Zařízení pro Vertikální Dopravu (In English: Systems and Machinery for Vertical Transport)*; ES ČVUT: Praha, Czech Republic, 1991; p. 139.
31. *ČSN EN 81-20*; Bezpečnostní Předpisy pro Konstrukci a Montáž Výtahů-Výtahy pro Dopravu Osob a Nákladů-Část 20: Výtahy pro Dopravu Osob a Osob a Nákladů (In English: Safety Rules for the Construction and Installation of lifts-Lifts for the Transport of Persons and Goods—Part 20: Passenger and Goods Passenger Lifts). CTN Unie Výtahového Průmyslu ČR: Praha, Czech Republic, 2015. Available online: https://www.technicke-normy-csn.cz/csn-en-81-20-274003-173799.html (accessed on 18 March 2016).
32. *ČSN EN 81-50*; Bezpečnostní Předpisy pro Konstrukci a Montáž Výtahů—Přezkoušení a Zkoušky—Část 50: Konstrukční Zásady. Výpočty. Přezkoušení a Zkoušky Výtahových Komponent (In English: Safety Rules for the Construction and Installation of Lifts—Examinations and Tests—Part 50: Design Rules. Calculations. Examinations and Tests of Lift Components). CTN Unie Výtahového Průmyslu ČR: Praha, Czech Republic, 2015. Available online: https://www.technicke-normy-csn.cz/csn-en-81-50-274003-173827.html (accessed on 17 January 2016).
33. *ČSN EN 81-71+AC*; Bezpečnostní Předpisy pro Konstrukci a Montáž Výtahů—Zvláštní Úpravy Výtahů Určených pro Dopravu Osob a Osob a Nákladů—Část 71: Výtahy Odolné Vandalům (In English: Safety Rules for the Construction and Installation of Lifts—Particular Applications to Passenger Lifts and Goods Lifts—Part 71: Vandal Resistant Lifts). ÚNMZ: Praha, Czech Republic, 2020. Available online: https://www.technicke-normy-csn.cz/csn-en-81-71-a1-274003-173845.html (accessed on 28 June 2019).
34. RSSC Load Cell 2020. Available online: https://www.hbm.cz/produkty/taho-tlakove-snimace-zatizeni/rscc/ (accessed on 11 September 2007).
35. Worm Gear Units 2007. Available online: http://www.sjt-moldava.sk/dokumenty/TS-Katalog.pdf (accessed on 11 March 2020).
36. Cvekl, Z.; Drazan, F. *Teoretické Základy Transportních Zařízení (In English: Theoretical Foundations of Transport Equipment)*; SNTL/ALFA: Praha, Czech Republic, 1976.